Vol. **121** (2012) *ACTA PHYSICA POLONICA A* No. 5–6

Proceedings of the European Conference Physics of Magnetism 2011 (PM'11), Poznań, June 27–July 1, 2011

Phase Composition and Magnetic Properties of Nanoperm Thin Films Doped with Yttrium

K. Brzózka[a,*], P. Sovák[b], T. Szumiata[a], B. Górka[a] and M. Gawroński[a]

[a]Department of Physics, Technical University of Radom, I. Krasickiego 54, 26-600 Radom, Poland

[b]Institute of Physics, P.J. Šafárik University, Park Angelinum 9, 041 54 Košice, Slovakia

Thin films of Nanoperm alloys with partial substitution of iron by yttrium are the subject of investigations. The attention is fixed on the influence of yttrium substitution on structure and magnetic characteristics of the samples. The effect of film thickness is also considered. Conversion electron Mössbauer spectroscopy and magneto-optic Kerr effect were used to derive hyperfine parameters and coercive field, respectively. Coexistence of crystalline bcc-Fe phase and an amorphous one with diverse proportion was stated in most of the samples. It was found that surface and interface regions contribute to the magnetic properties of films.

PACS: 75.50.Bb, 75.70.–i, 76.80.+y, 78.20.Ls

1. Introduction

Amorphous and nanocrystalline alloys based on iron, in form of ribbons, are known for their excellent soft magnetic properties [1]. Especially, materials belonging to so-called Finemet family (Fe–Cu–Nb–Si–B) and Nanoperm one (Fe–Zr/Nb/–B/Cu/) are useful for applications in electronics, electrical engineering and other fields of technology [2]. Manufacture of alloys of similar chemical composition in form of thin films gives additional possibility of applications, e.g. in microelectronics. Furthermore, structural and magnetic properties of thin films can differ from the ribbon ones due to another preparation method and considerable fraction of surface regions. This makes motivation for studying various kinds of thin films with slightly modified composition in comparison to bulk counterparts.

Between others, transition metal elements, partially substituting iron, are good candidates for modification of structural and magnetic properties of Nanoperm. It was reported that in Nanoperm ribbons yttrium addition accelerates nucleation of crystal growth and causes a slowing down of diffusion processes in relation to the Y free alloy and, consequently, affects their characteristics [3]. Moreover, changes in magnetic properties, microstructure and thermal stability caused by Y substitution of some $Fe_{81}Zr_7B_5Y_7$ thin films were also found [4]. This is why a more systematic study of this problem was undertaken.

2. Experimental details

Samples of composition $Fe_{88-x}Zr_7B_5Y_x$ ($x = 1, 5, 9, 12$) and various thickness belonging to the range ($20 \div 150$) nm were produced by flash evaporation under ultrahigh vacuum and by subsequent deposition onto a liquid nitrogen cooled substrate. Conversion electron Mössbauer spectroscopy (CEMS) measurements were carried out by means of ^{57}Co(Rh) source of gamma radiation placed on a vibrator working in a conventional constant acceleration mode. For electron detection, a gas-flow counter supplied with He+4%CH_4 mixture was employed. The Mössbauer spectra were resolved by use of the NORMOS software. Hysteresis loops were recorded with a magneto-optic Kerr effect (MOKE) system consisting of a red laser diode, a foil polarizer, a half-wave plate, a Wollaston prism, two-photodiode differential detector and a coreless magnetizing coil supplied with 50 Hz current. External magnetic field of magnitude of several mT was applied in-plane of the film. Both MOKE signal from detector and coil current were registered by use of an oscilloscope. The measurements were carried out for various orientations of the sample axis.

3. Results

3.1. Mössbauer spectrometry

The Mössbauer spectra of selected thin films are shown in Fig. 1a–c, Fig. 2a–c. Their complex shape reveals multi-phase character of most of investigated films. A sharp sextet with magnetic hyperfine field (MHF) equal to 33.0(±0.1) T and isomer shift $\delta = 0.00(\pm 0.01)$ mm/s dominates in all spectra collected for alloys with yttrium content $x < 9$ at.% (independently of the film thickness) which points to the significant content of polycrystalline (or nanocrystalline) bcc-Fe phase.

No indications of yttrium presence inside the crystallites are found in the spectra. In addition, components with distributed hyperfine parameters occur: (i) a high-field sextet with distributed MHF larger than 18 T and isomer shift about 0.04 mm/s, (ii) a low-field sextet with distributed MHF belonging to the range ($5 \div 20$) T and isomer shift about 0.4 mm/s, (iii) a doublet with distributed quadrupole splitting (QS) from the range (0, 1.2) mm/s and isomer shift about 0.4 mm/s (Fig. 3).

---

[*] corresponding author; e-mail: `k.brzozka@pr.radom.pl`

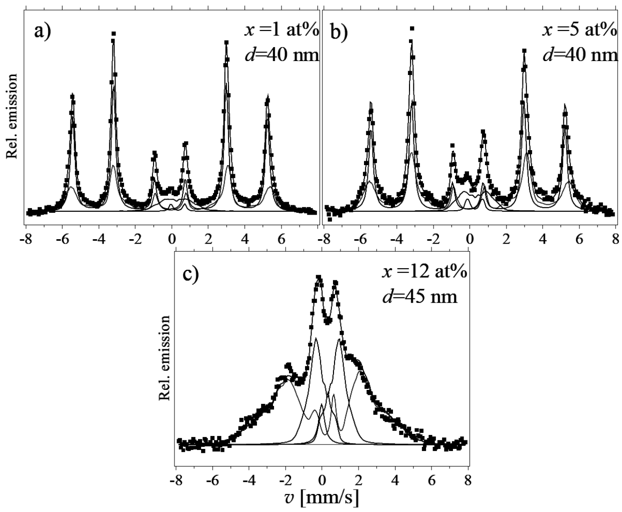

Fig. 1. CEMS spectra (and their components) collected for selected samples of similar thickness, $d = (40 \div 45)$ nm, and different content of yttrium: $x = 1$ at.% (a), $x = 5$ at.% (b), $x = 12$ at.% (c).

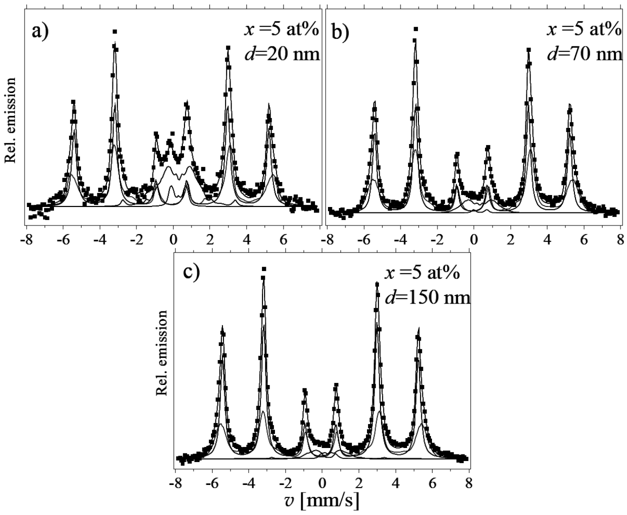

Fig. 2. CEMS spectra (and their components) collected for selected samples of similar yttrium percentage ($x = 5$ at.%) and different thickness: $d = 20$ nm (a), $d = 40$ nm (b), $d = 150$ nm (c).

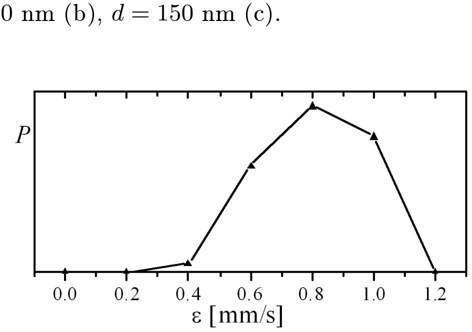

Fig. 3. Quadrupole splitting distribution derived for $Fe_{83}Zr_7B_5Y_5$ thin film of thickness 40 nm.

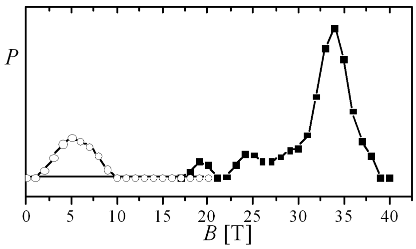

Fig. 4. MHF distribution derived for $Fe_{83}Zr_7B_5Y_5$ thin film of thickness 40 nm: open circles — a low-field part, closed squares — a high-field one.

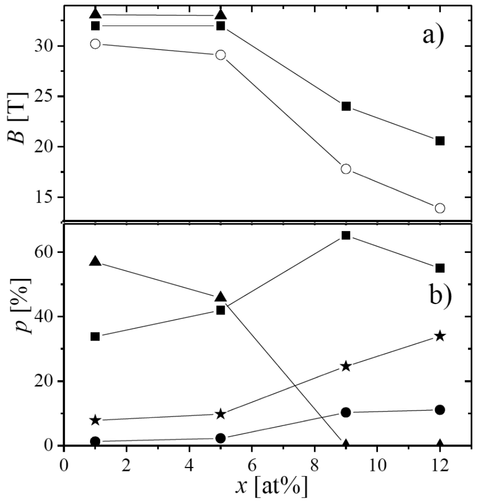

Fig. 5. Open circles — mean MHF over the whole sample (a), squares — mean MHF (a) and percentage (b) of the high-field part of MHF distribution, triangles — MHF (a) and percentage (b) of the sextet related to bcc-Fe, stars — percentage of the low-field part of MHF distribution (b), full circles — percentage of the paramagnetic component (b), as a function of yttrium atomic content (thickness of films $d = 40 \div 45$ nm).

Typical MHF distribution, comprising components (i) and (ii), is shown in Fig. 4. The main part of the distribution contains a well-marked maximum about 34 T which can be attributed to the surface of crystallites and interfaces. The presence of hyperfine field values higher than 33.3 T (typical for bulk Fe) presumably is a sign of enhancement of MHF at Fe/metal interfaces observed sometimes in thin layers [5] due to the breakdown of translational symmetry. Besides, considerable mechanical strain can additionally widen the magnetic hyperfine field distribution. The other parts of MHF distribution, mainly low-field ones, as well as the paramagnetic subspectrum, are related to an amorphous phase, which is strongly inhomogeneous. Particularly, the paramagnetic doublet may originate from amorphous regions rich in yttrium; iron atoms situated at the surface of the thin film can also contribute to this component. Samples with $x = 9$, 12, $d = 40$ nm seem to be fully amorphous,

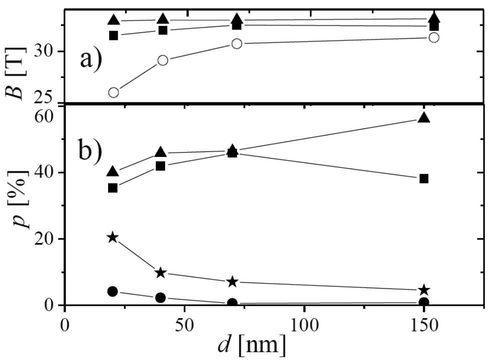

Fig. 6. Open circles — mean MHF over the whole sample (a), squares — mean MHF (a) and percentage (b) of the high-field part of MHF distribution, triangles — MHF (a) and percentage (b) of the sextet related to bcc-Fe, stars — percentage of the low-field part of MHF distribution (b), full circles — percentage of the paramagnetic component (b), as a function of film thickness (yttrium content $x = 5$ at.%).

with significant contribution of paramagnetic component (Fig. 1c).

The above presented interpretation of the Mössbauer spectra is confirmed by the dependences of MHF and relative percentage of the components on yttrium content, x, and film thickness, d. These relationships are plotted in Fig. 5a,b and Fig. 6a,b, respectively. Moreover, we can notice that mean MHF is a decreasing function of x.

3.2. MOKE magnetometry

MOKE hysteresis loops were measured at magnetic field parallel to in-plane easy-axes, whose directions were not strictly correlated with the substrate edges (which points to the substantial strain contribution to the magnetocrystalline anisotropy).

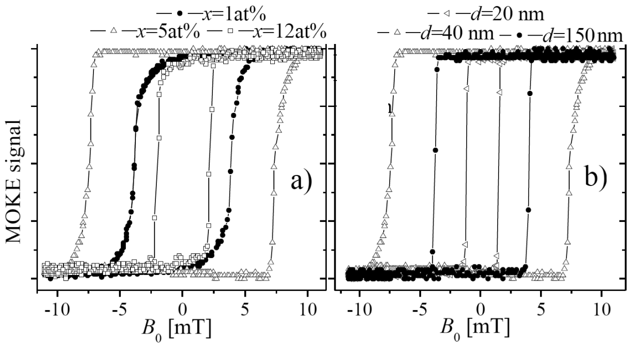

Fig. 7. MOKE curves measured for $Fe_{88-x}Zr_7B_5Y_x$ thin films of different yttrium concentration (a) and different film thickness (b).

Figure 7a,b presents an evolution of the curves with yttrium content and film thickness, respectively. In the series of samples of near constant thickness (40÷45 nm) a minimal induction of the coercive field (≈ 2.1 mT) is observed for the sample of maximal yttrium content. This proves the weakening of magnetic interactions with significant yttrium addition and is related to the drop of average hyperfine magnetic field observed in CEMS experiment as well as increasing contribution of the amorphous phase. In the case of samples of fixed Y concentration (5 at.%) the thickest sample ($d = 150$ nm) is characterized by the minimal induction of the coercive field (≈ 1.3 mT). This could be interpreted as a consequence of higher "strain resistance" of the thick film. In both series, the 40 nm thick sample containing 5 at.% of yttrium reveals the maximal coercivity (7.4 mT). It could be explained by possible forming of high-coercivity phases ($Fe_{17}Y_2$, $Fe_{23}Y_6$, Fe_3Y, Fe_2Y [6, 7]) for this specific yttrium concentration. Traces of such phases can be seen in Fig. 4 in the form of additional peaks in the MHF distribution at 19 T and 24 T.

4. Summary

Thin films of composition $Fe_{88-x}Zr_7B_5Y_x$ were investigated by conversion electron Mössbauer spectroscopy and MOKE magnetometry. It was stated that film structure strongly depends on yttrium concentration: coexistence of bcc-Fe and an amorphous phase is observed for $x < 9$ but for $x \geq 9$ the alloys are almost fully amorphous. The surface and interface effects were also observed. It was found that mean magnetic hyperfine field is a decreasing function of x. The coercivity of the investigated films equals several mT (up to maximal value of 7.4 mT). Moreover, it changes non-monotonically with yttrium concentration and film thickness.

References

[1] G. Herzer, *Phys. Scr. T* **49**, 307 (1993).

[2] M.E. McHenry, D.E. Laughlin, *Acta Mater.* **48**, 223 (2000).

[3] A. Chrobak, V. Nosenko, G. Haneczok, L. Boichyshyn, M. Karolus, B. Kotur, *J. Non-Cryst. Solids* **357**, 4 (2011).

[4] I. Gościańska, T. Toliński, J. Dubowik, H. Ratajczak, P. Sovak, M. Konč, *Czech. J. Phys.* **52**, A185 (2002).

[5] F. Klinkhammer, Ch. Sauer, E.Yu. Tsymbal, S. Handschuh, Q. Leng, W. Zinn, *J. Magn. Magn. Mater.* **161**, 49 (1996).

[6] W. Zhang, G. Liu, K. Han, *J. Phase Equilibria* **13**, 304 (1992).

[7] A. Venskutonis, F. Aubertin, J. Breme, *Hyperfine Interact.* **112**, 161 (1998).